

The effect of Phase Composition on the Photocatalytic Activity of Cu₂O/CuO/Cu Composites for Methylene Blue Photodegradation

Mokhammad Ali Rizqi Maulana¹, Aisyaturridha¹, Bimo TriGoutomo², Amir Mahmud^{3,*}

¹The Center for Science Innovation, No. 40 BC Arva Building, Jl. RP. Soeroso, Jakarta Pusat 10350, Indonesia

²Department of Environmental Engineering, Pukyong National University, Yongso-ro, Busan, Korea

³Division of Chemical Convergence Engineering, Pukyong National University, Yongso-ro, Busan, Korea

*Corresponding author: amirmahmud@pukyong.ac.kr

Received

5 December 2024

Received in revised form

3 January 2025

Accepted

3 January 2025

Published online

28 February 2025

DOI

<https://doi.org/10.56425/cma.v4i1.87>



Original content from this work may be used under the terms of the [Creative Commons Attribution 4.0 International License](https://creativecommons.org/licenses/by/4.0/).

Abstract

This study investigates the influence of phase composition on Cu₂O/CuO/Cu composites for the degradation methylene blue (MB) under visible light irradiation. Two types of composites, Cu₂O-rich and Cu₂O-poor, were successfully synthesized through electrodeposition method. The results showed that the Cu₂O-rich composite exhibited photocatalytic activity, as indicated by a maximum photocurrent of 13 mA/cm² and the highest optimized MB photodegradation efficiency. This enhanced performance is due to the high Cu₂O phase content, which generates a higher photocurrent density, thereby accelerating the redox reaction in the MB degradation.

Keywords: Cu₂O/CuO/Cu composite, phase composition, photodegradation

1. Introduction

Methylene blue (MB) is a synthetic dye that has an aromatic molecular structure, which makes it resistant to biodegradation [1]. As a result, these dye wastes can accumulate in the environment at high concentrations [2]. Careless disposal of MB waste into the environment, especially in the aquatic environment threatens the life of aquatic ecosystems [3]. MB waste in high concentrations is also dangerous for the health of the human body, causing various problems from digestive disorders to damage to vital organs [4,5]. Therefore, MB waste treatment is needed to maintain environmental quality and health [6].

Degradation methods with photocatalytic processes have been shown to be effective in decomposing dyes [7,8]. This technique utilizes photocatalysts exposed to light to generate electron-hole pairs, which then react with water to form oxygen and hydroxyl radicals [9]. These radicals are able to oxidize organic compounds into simple molecules such as CO₂ and H₂O [10]. Photocatalytic processes are known to be cost-effective, efficient, and capable of degrading various types of dyes, including MB [11,12]. The degradation efficiency is highly dependent on

the photocatalyst used, which can be optimized by improving the physical, optical, and electronic properties of the material [13].

A promising catalyst is copper-based metal oxides, such as cuprous oxide (Cu₂O) and cupric oxide (CuO) [14]. Both of these materials have relatively narrow band gaps semiconductors, which are 2.0-2.5 eV for Cu₂O and 1.2-1.7 eV for CuO [15]. The small band gap allows these materials to absorb the visible light spectrum well. In addition, both have good chemical stability, non-toxic, and abundant in nature [14].

Composite Cu₂O/CuO shows a significant synergistic effect. This combination increases the charge transfer efficiency due to the potential difference between the conduction and valence bands of both materials [16]. In this photocatalyst scheme, the electrons generated by Cu₂O are efficiently transferred to CuO. However, electron injection from Cu₂O/CuO to the solution is often limited by slow kinetics and self-reduction of CuO by accumulated electrons [17]. The addition of Cu metal has been reported to be effective for accelerating electron transfer and overcoming these limitations.

The purpose of this study is to evaluate the effect of Cu₂O/CuO/Cu composite phase composition on photocatalytic activity in MB degradation. The results showed that a higher Cu₂O phase content significantly increased the photocurrent density and resulted in a greater percentage of MB photodegradation. This study provides insight into how the influence of Cu₂O phase composition in the enhancement of composite photocatalyst activity. In addition, it provides knowledge about efficient synthesis routes in the preparation of composites.

2. Materials and Method

2.1 Materials

The pro-analyst chemicals used were copper sulfate pentahydrate (CuSO₄·5H₂O), sodium sulfate (Na₂SO₄), lactic acid (C₃H₆O₃), sodium hydroxide (NaOH), and methylene blue (C₁₆H₁₈ClN₃S) were all supplied from Merck.

2.2 Methods

2.2.1 Synthesize of Cu₂O/CuO/Cu

Composite synthesis was carried out via electrodeposition method. The electrolyte solution was prepared by dissolving 0.312 g CuSO₄·5H₂O, 6,3 mL C₃H₆O₃, and 0.71 M Na₂SO₄ in distilled water. The composition of Cu₂O in the composite was adjusted by adjusting the pH of the electrolyte: pH 11 for Cu₂O-rich composite and pH 9 for Cu₂O-poor composite. The pH value was adjusted by the addition of 10 M NaOH solution. The electrodeposition process was carried out at a potential of -0.3 V vs Ag/AgCl for 60 minutes with a deposition temperature of 50°C. After the process was completed, the composite film was cleaned and dried at room temperature.

2.2.2 Characterizations

The phase fraction of Cu₂O/CuO/Cu composite was analyzed using an X-ray diffractometer (XRD, Bruker D8 Advance Eco with Lynxeye XE-T Cu Source). While morphology analysis uses a scanning electron microscope (SEM, Carl Zeiss EVO 10).

2.2.3 Electrochemical tests

Electrochemical impedance (EIS) and photoelectrochemical (PEC) tests were conducted to evaluate the performance of the composite samples. EIS measurements were performed in the frequency range of 0.1 Hz to 100 kHz and amplitude of 10 mV, used to measure the charge transfer resistance (*R_{ct}*). Meanwhile, PEC measurements were performed in the potential range of -

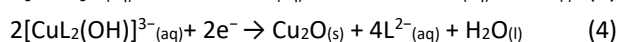
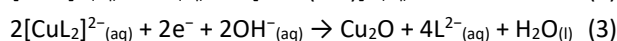
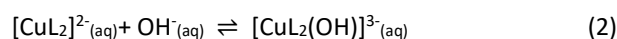
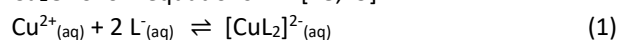
0.1 V to 0.45 V vs Ag/AgCl to measure the photocurrent density. All tests were performed in 1 M Na₂SO₄ solution. During the test, the composite was illuminated by halogen lamp solar simulator AM 1.5 G.

2.2.4 Photocatalytic activity test

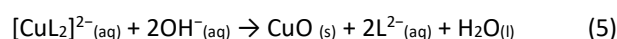
The photocatalyst activity was assayed by degrading 5 ppm MB 10 mL measured under the irradiation of halogen lamp solar simulator AM 1.5 G. The degradation MB was determined by measuring the absorbance at a wavelength of 664 nm using a UV-VIS spectrophotometer (GB Cintra Ver. 2.4). The test was conducted for 2 hours.

3. Results and Discussion

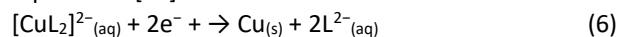
The electrodeposition process of Cu₂O/CuO/Cu composite in base electrolyte is carried out by complexing lactate ions. The lactate ions came from a deprotonation reaction during the presence of a base. Copper ions (Cu²⁺) react with lactic acid ions to form a complex, where Cu²⁺ as the central atom binds to two deprotonized lactic acid molecular ions [CuL₂]²⁻. Cu²⁺ species are stabilized in the alkaline solution and diffuse during the coating process to the surface of the working electrode, where the ions undergo release and deposition. The cathodic reduction of copper lactate ions [CuL₂]²⁻ to Cu₂O, CuO, and Cu is strongly influenced by pH or hydroxide ion (OH⁻) concentration. The possible reactions in the reduction of copper lactate to Cu₂O follow equations 1-4 [18,19].



While for the formation of CuO, the deposition reaction that occurs follows equation 5 [20,21].



During the deposition process, the pH value decreases due to the consumption of OH⁻ in the solution. Under these conditions, the Cu metal phase is formed following equation 6 [22].



3.1 Phase analysis

Cu₂O/CuO/Cu composites have been successfully synthesized using the electrodeposition method, which was identified through XRD analysis. Figure 1 shows the diffraction pattern of the composite. Cu₂O phase peaks appear at 2θ 36.43°, 42.31°, 61.38°, and 73.53°, corresponding to (111), (200), (220), and (222) planes (ICSD No. 01-071-3645). The CuO phase peaks appear at 2θ

35.52°, 38.94°, 48.72°, and 56.66°, corresponding to (-111), (200), (-202), and (021) planes (ICSD No. 01-077-7717), respectively. Meanwhile, the Cu phase peak only appears at 2θ 43.31°, corresponding to the (111) plane (ICSD No. 01-085-1326).

Table 1. Phase fraction of composites Cu₂O/CuO/Cu.

Sample	Phase fraction (%)		
	Cu ₂ O	CuO	Cu
Cu ₂ O-rich	77	12	11
Cu ₂ O-poor	36	23	39

Based on the composition shown in Table 1, the fraction of the Cu₂O phase can be significantly increased by increasing the pH value. When the pH is increased to 11, it can be seen that the peak intensity of the Cu₂O phase increases, especially the peak of the (111) plane. The high and sharp diffraction intensity indicates that the (111) crystal surface grows optimally and has high crystallinity. These results are in accordance with previous studies showing that the orientation of the (111) Cu₂O plane is better at high solution pH [23,24].

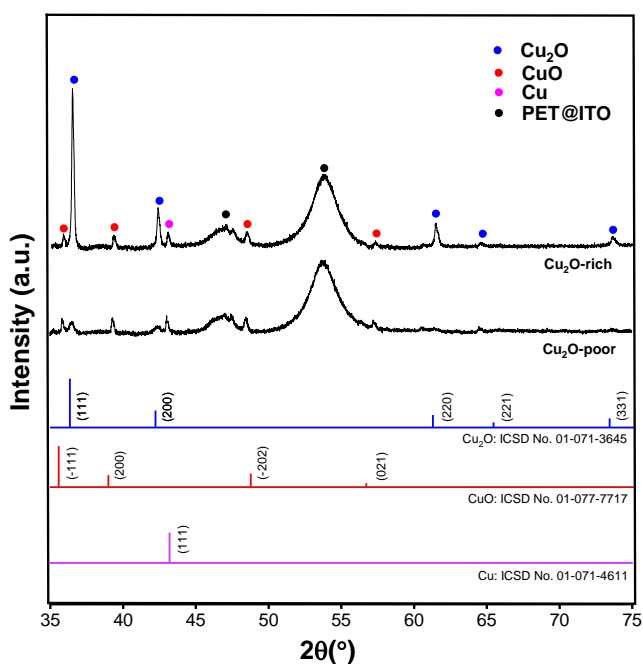


Figure 1. Diffractograms of Cu₂O-rich and Cu₂O-poor composites.

Cu₂O diffraction peaks at Cu₂O-poor relatively had a low intensity compared to Cu₂O-rich which was synthesized at higher pH. Meanwhile, the intensity of the Cu and CuO diffraction peaks decreased at the Cu₂O-rich. This shows that the formation of Cu₂O is thermodynamically preferred in alkaline electrolytes with higher pH values [25]. While the Cu phase becomes dominant as the deposition process progresses because

the concentration of OH⁻ ions decreases. So theoretically the reduction of the [CuL₂]²⁻ complex to Cu is preferred.

3.2 Morphological analysis

As observed in the SEM images presented in Fig. 2, there is a significant morphological difference between the Cu₂O-rich and Cu₂O-poor composites. The Cu₂O-rich composite shows an irregular surface structure with overlapping pyramid-like shapes. The particle size varies, but in general, tends to be larger than the sample at Cu₂O-poor [26]. The pyramidal shape indicates that crystal growth is more dominant in certain directions, namely in the (111) plane [24]. While the Cu₂O-poor composite shows a more uniform and compact structure compared to the sample.

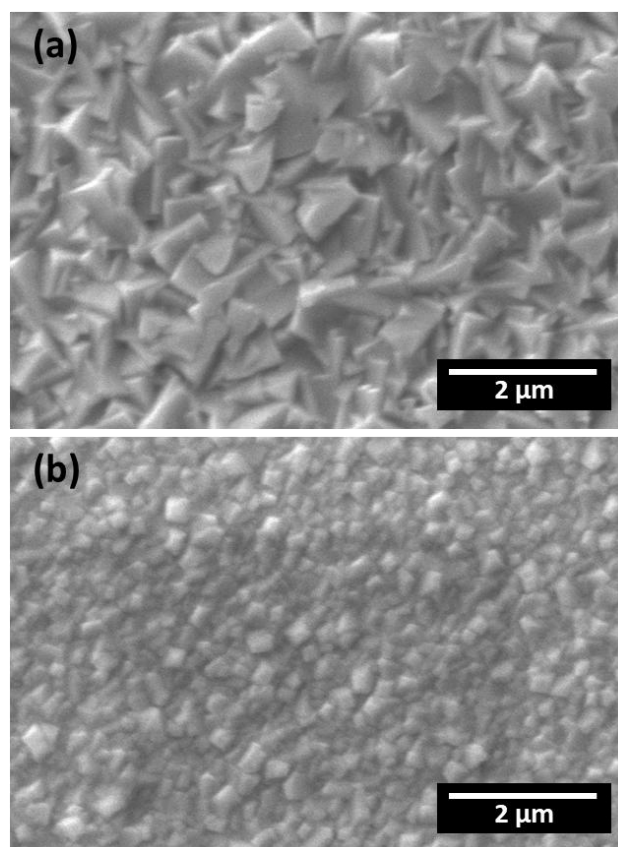


Figure 2. SEM micrographs of composite (a) Cu₂O-rich and (b) Cu₂O-poor.

3.3 Electrochemical analysis

The charge transfer efficiency of the composites was studied using EIS. Figure 3 shows the Nyquist plots of the Cu₂O-rich and Cu₂O-poor composites. The diameter of the semicircle on the Nyquist plot related to the magnitude of the charge transfer resistance [27]. The phase of the composite greatly influences the charge transfer process.

The composite with Cu₂O-poor, with a higher Cu content, had an R_{ct} value of 127 Ω . Otherwise, the Cu₂O-rich composite, with a higher Cu₂O oxide phase content, produced a larger transfer resistance value of 317 Ω . This is comparable with the electrical conductivity properties of each phase. Cu has better electrical conductivity than Cu₂O. In addition, the increased composition of the CuO phase in the sample Cu₂O-poor also contributes to the increased conductivity of the sample. CuO as known has a higher electrical conductivity compared to Cu₂O [28].

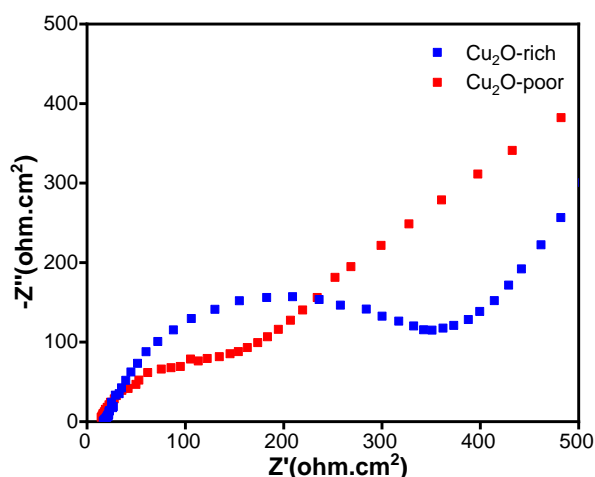


Figure 3. Nyquist plots of composite Cu₂O-rich and Cu₂O-poor.

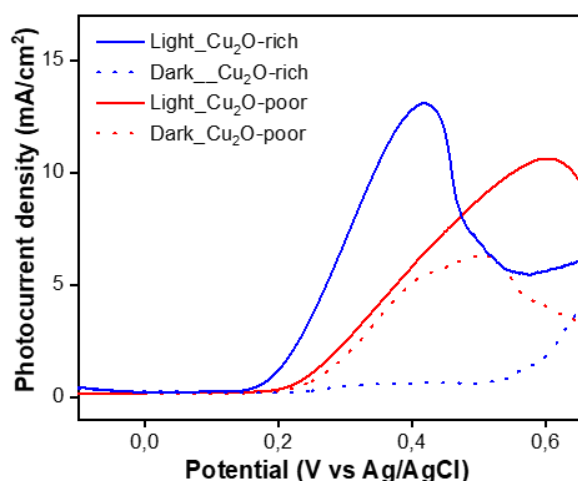


Figure 4. Linear sweep voltammetry curves were obtained for composites Cu₂O-rich and Cu₂O-poor. The measurement was conducted under both light (solid line) and dark conditions (dotes line).

Under the PEC test, composite samples are irradiated with visible light to produce a current due to the photoelectric effect derived from electron excitation in the oxide phase [29]. This test relates the potential applied to

the sample with the resulting photocurrent density under illumination [30]. In the dark condition test, the Cu₂O-rich composite produces a low current response, as shown in Fig. 4. Conversely, a Cu₂O-poor composite, which contains higher Cu, produces larger currents because Cu is a conductive material.

The Cu₂O-rich composite also produces a larger current response in light conditions. This happens because the higher oxide phase creates a more photogenerated charge. Evidently, the maximum photocurrent of Cu₂O-rich composite reaches 13.1 mA/cm² at 0.4 V vs Ag/AgCl. Meanwhile, the maximum photocurrent generated by the composite Cu₂O-poor only reached 6.1 mA/cm² at 0.4 V vs Ag/AgCl.

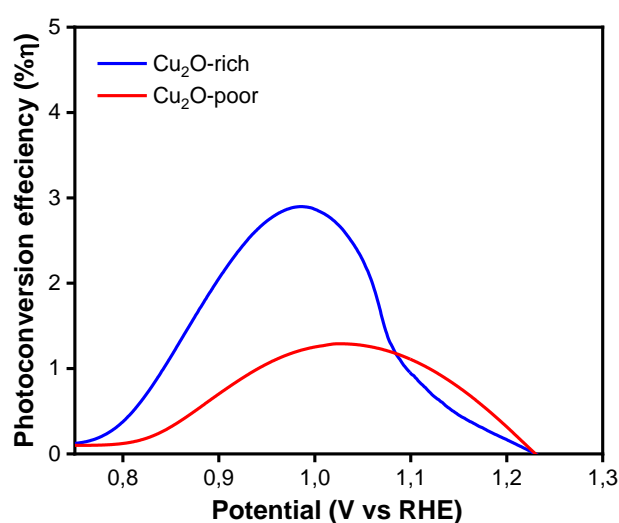


Figure 5. The plot of energy conversion efficiency (% η) versus applied potential (RHE).

Photoconversion efficiency is calculated to evaluate the efficiency of the composite in converting light energy into electrical energy. Photoconversion is calculated through the following equation (7).

$$\eta\% = J_p \times \left(\frac{E_{rev} - |E_{app}|}{I_{light}} \right) \times 100\% \quad (7)$$

Where J_p is the photocurrent density, E_{rev} is the reference potential in this case 1.23 vs RHE (reversible hydrogen electrode), E_{app} is the applied potential vs RHE, and I_{light} is the solar simulator light intensity (100 w/cm²). Additionally, the conversion of RHE units to Ag/AgCl follows the following equation (8).

$$E_{RHE} = E_{Ag/AgCl} + 0,059 \times pH + 0.197 \quad (8)$$

As presented in Fig. 5, photoconversion efficiency demonstrates that Cu₂O-rich composites exhibit relatively higher efficiency than Cu₂O-poor composites at lower potentials, primarily attributed to the significantly higher photocurrent density generated by the Cu₂O-rich sample.

3.4 Photodegradation performances

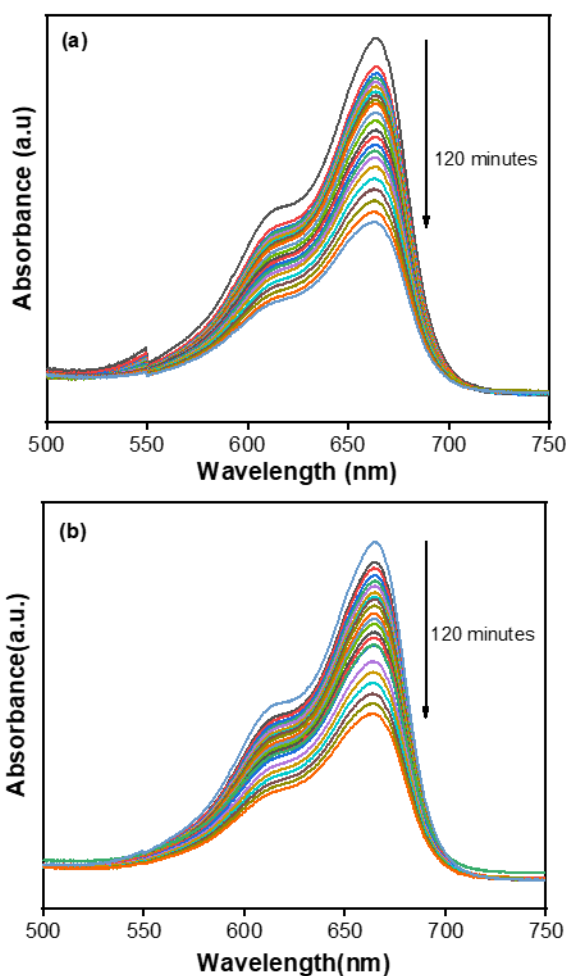


Figure 6. UV-Vis spectra measured during methylene blue photodegradation using $\text{Cu}_2\text{O}/\text{CuO}/\text{Cu}$ synthesized at different pH values (a) Cu_2O -rich and (b) Cu_2O -poor.

The photocatalytic performance of the composite was assessed from the photodegradation of MB under visible light irradiation. As presented in Fig. 6, the absorbance of MB decreased in line with time, which indicates desirable degradation processes. When the composite is exposed to photons ($h\nu \leq \text{nm}$) with energy equal to or greater than the band gap energy, electrons (e^-) in the Cu_2O valence band will be excited to the conduction band and then move to the CuO conduction band. Meanwhile, the holes (h^+) from CuO move to the Cu_2O valence band. This charge transfer separates electron-hole pairs efficiently, thereby improving catalytic performance [31]. However, the electron transfer process from the composite to the solution can be hindered by poor contact or structural defects, which cause electrons to accumulate and cause photoreduction of the sample [17]. Photoreduction should be avoided because it can interfere with the performance and stability of the

photocatalyst. Therefore, Cu metal is used to enhance electron transfer as the metal has good conductive properties. The schematic mechanism of photodegradation MB is demonstrated in Fig. 7.

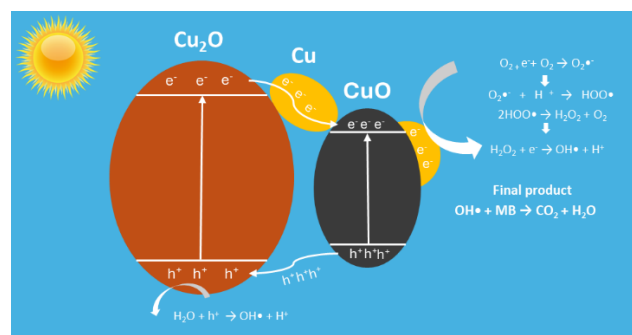


Figure 7. Schematic photodegradation MB using composite $\text{Cu}_2\text{O}/\text{CuO}/\text{Cu}$.

The electron and hole pairs produced by the composite then participate in the degradation reaction of MB. Based on Budi et al. [9] the photodegradation reaction mechanism can be written as follows.

Absorption of photons:



Oxygen reduction to superoxide anion:



Protonation superoxide anion to hydroperoxyl radicals and then subsequently form peroxide:



Dissociate peroxide to hydroxyl radical:



Oxidation water to hydroxyl radical:



MB degradation to water and carbon dioxide using radical hydroxyl:



As shown in Fig. 8a, the percentage degradation of MB increases as the irradiation time. This photocatalytic reaction follows a pseudo-first-order, as indicated by the strong linear correlation between $\ln(C_0/C)$ and irradiation time, following previous research reports, Fig. 8b [8]. The test results showed that the Cu_2O -rich composite sample achieved an MB degradation percentage of 48%, higher than the Cu_2O -poor composite sample which only reached 46%. This difference in photocatalytic performance can be explained by the ability of the Cu_2O -rich sample to produce more photo charges. The higher the number of photo charges generated, the freer radicals are formed to oxidize the MB molecules. Thus, the resulting percentage of MB degradation is also higher [32]. This degradation

percentage achievement is relatively higher than the $\text{Cu}_2\text{O}/\text{Cu}$ composite reported by previous research which only reached around 20% in the same reaction time [9].

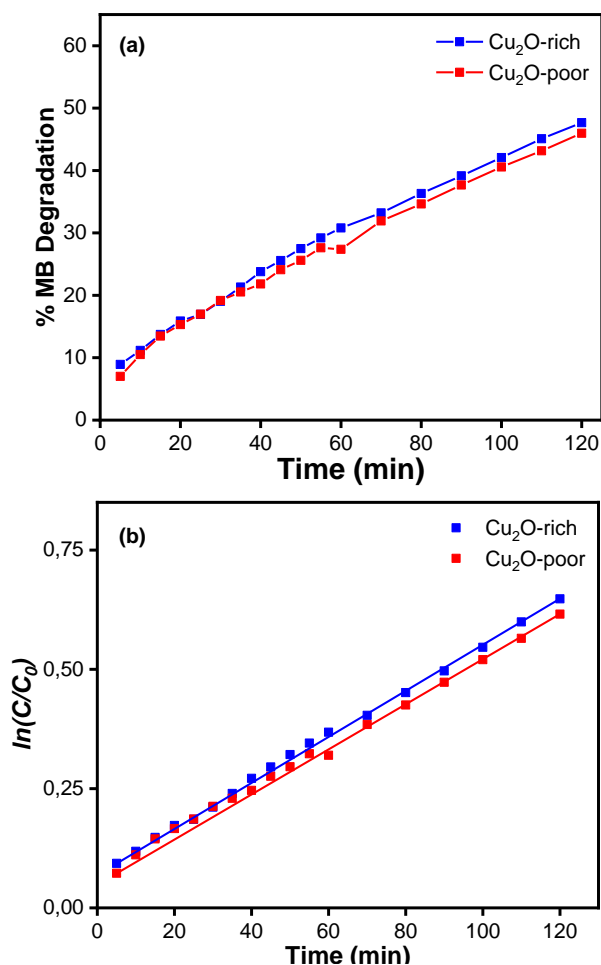


Figure 8. (a) Photodegradation of methylene blue was performed under light irradiation using $\text{Cu}_2\text{O}@/\text{CuO}@/\text{Cu}$ and (b) photocatalytic reaction curves.

4. Conclusion

$\text{Cu}_2\text{O}/\text{CuO}/\text{Cu}$ composite was successfully synthesized using the electrodeposition method. The phase fraction of the composite is controlled by adjusting the pH. The Cu_2O fraction plays an important role in increasing the photocurrent density and photocatalytic activity of MB due to increased charge photogeneration.

Author contributions

Mokhammad Ali Rizqi Maulana: Writing Original Draft, Conceptualization, Methodology, Validation, Formal Analysis. Aisyaturridha: Writing Original Draft, Investigation, Data Curation, Visualization. Bimo

TriGuotomo: Writing-Review & Editing & Supervision. Amir Mahmud: Writing-Review & Editing & Supervision.

Conflicts of interest

There are no conflicts to declare.

Acknowledgement

This research was funded by the Directorate of Research, Technology, and Higher Education (DRTPM), Ministry of Education, Culture, Research, and Technology of the Republic of Indonesia, through the third-year Applied Research scheme for the fiscal year 2024.

References

- [1] M. Saeed, M. Muneer, A. ul Haq, N. Akram, Photocatalysis: an effective tool for photodegradation of dyes—a review, *Environmental Science and Pollution Research*. **29** (2022) 293–311. <https://doi.org/10.1007/s11356-021-16389-7>.
- [2] N.P. Rini, N.I. Istiqomah, Sunarta, E. Suharyadi, Enhancing photodegradation of methylene blue and reusability using CoO/ZnO composite nanoparticles, *Case Studies in Chemical and Environmental Engineering*. **7** (2023) 100301. <https://doi.org/10.1016/j.cscee.2023.100301>.
- [3] T.A. Kurniawan, Z. Mengting, D. Fu, S.K. Yeap, M.H.D. Othman, R. Avtar, T. Ouyang, Functionalizing TiO_2 with graphene oxide for enhancing photocatalytic degradation of methylene blue (MB) in contaminated wastewater, *J Environ Manage*. **270** (2020) 110871. <https://doi.org/10.1016/j.jenvman.2020.110871>.
- [4] M.S.I. Nasri, M.F.R. Samsudin, A.A. Tahir, S. Sufian, Effect of MXene Loaded on g-C $_3$ N $_4$ Photocatalyst for the Photocatalytic Degradation of Methylene Blue, *Energies (Basel)*. **15** (2022) 955. <https://doi.org/10.3390/en15030955>.
- [5] I. Khan, K. Saeed, I. Zekker, B. Zhang, A.H. Hendi, A. Ahmad, S. Ahmad, N. Zada, H. Ahmad, L.A. Shah, T. Shah, I. Khan, Review on Methylene Blue: Its Properties, Uses, Toxicity and Photodegradation, *Water (Switzerland)*. **14** (2022). <https://doi.org/10.3390/w14020242>.
- [6] J. Akter, K.P. Sapkota, Md.A. Hanif, Md.A. Islam, H.G. Abbas, J.R. Hahn, Kinetically controlled selective synthesis of Cu_2O and CuO nanoparticles toward enhanced degradation of methylene blue using ultraviolet and sun light, *Mater Sci Semicond Process*. **123** (2021) 105570.

- <https://doi.org/https://doi.org/10.1016/j.mssp.2020.105570>.
- [7] S. Budi, M. Takahashi, M.G. Sutrisno, W.A. Adi, Z. Fairuza, B. Kurniawan, S. Maenosono, A.A. Umar, Phases evolution and photocatalytic activity of Cu₂O films electrodeposited from a non-pH-adjusted solution, *R Soc Open Sci.* **10** (2023). <https://doi.org/10.1098/rsos.230247>.
- [8] Muhamad Athariq, Muhammad Raihan Rauf, Ikhfa Wiqoy Khairany, Intan Fadia Adani, Mega Gladiani Sutrisno, Synthesis and Characterization of Nanocube Cu₂O Thin Film at Room Temperature for Methylene Blue Photodegradation Application, *Chemistry and Materials.* **2** (2023) 67–71. <https://doi.org/10.56425/cma.v2i3.65>.
- [9] S. Budi, M. Gladiani Sutrisno, T. Hadinugrahaningsih, Synergistic enhancement of photocatalytic efficiency and durability in CoNi-decorated Cu₂O/Cu films for superior synthetic dye degradation, *Cleaner Materials.* **12** (2024) 100250. <https://doi.org/10.1016/j.clema.2024.100250>.
- [10] M.A. Rizqi Maulana, Aisyaturridha, Salmah Cholilah, F. Dwi Arista, Bagus Nur Listiyono, Nickel Oxide (NiO) Thin Film Synthesis via Electrodeposition for Methylene Blue Photodegradation, *Chemistry and Materials.* **2** (2023) 61–66. <https://doi.org/10.56425/cma.v2i3.62>.
- [11] S. Budi, M.G. Sutrisno, Y. Pratiwi, N. Yusmaniar, Enhanced photocatalytic activity of CoNi-decorated Zn-doped Cu₂O synthesized by electrodeposition technique, *Mater Adv.* **4** (2023) 1081–1088. <https://doi.org/10.1039/d2ma00916a>.
- [12] S. Budi, M. Takahashi, M.G. Sutrisno, W.A. Adi, Z. Fairuza, B. Kurniawan, S. Maenosono, A.A. Umar, Phases evolution and photocatalytic activity of Cu₂O films electrodeposited from a non-pH-adjusted solution, *R Soc Open Sci.* **10** (2023). <https://doi.org/10.1098/rsos.230247>.
- [13] P. Kumari, A. Kumar, ADVANCED OXIDATION PROCESS: A remediation technique for organic and non-biodegradable pollutant, *Results in Surfaces and Interfaces.* **11** (2023) 100122. <https://doi.org/10.1016/j.rsurfi.2023.100122>.
- [14] M.S.S. Danish, L.L. Estrella, I.M.A. Alemaida, A. Lisin, N. Moiseev, M. Ahmadi, M. Nazari, M. Wali, H. Zaheb, T. Senjyu, Photocatalytic applications of metal oxides for sustainable environmental remediation, *Metals (Basel).* **11** (2021) 1–25. <https://doi.org/10.3390/met11010080>.
- [15] C.D. Sai, V.T. Pham, T.N.A. Tran, T.T.H. Tran, T.B.N. Vu, T.H.H. Hoang, A.S. Pham, T.M.T. Nguyen, T.T.H. Duong, H.H. Do, Construction of Highly Condensed Cu₂O/CuO Composites on Cu Sheet and Its Photocatalytic in Photodegradation of Hazardous Colouring Agent Rose Bengal, *Mater Trans.* **64** (2023) 2134–2142. <https://doi.org/10.2320/matertrans.MT-MG2022008>.
- [16] A. Khataee, D. Kalderis, P. Gholami, A. Fazli, M. Moschogiannaki, V. Binas, M. Lykaki, M. Konsolakis, Cu₂O-CuO@biochar composite: Synthesis, characterization and its efficient photocatalytic performance, *Appl Surf Sci.* **498** (2019) 143846. <https://doi.org/10.1016/j.apsusc.2019.143846>.
- [17] S. Mosleh, M.R. Rahimi, M. Ghaedi, K. Dashtian, S. Hajati, Sonochemical-assisted synthesis of CuO/Cu₂O/Cu nanoparticles as efficient photocatalyst for simultaneous degradation of pollutant dyes in rotating packed bed reactor: LED illumination and central composite design optimization, *Ultrason Sonochem.* **40** (2018) 601–610. <https://doi.org/10.1016/j.ultsonch.2017.08.007>.
- [18] S. Budi, D.I. Syafei, Electrodeposition of Zn Zn-doped Cu Cu₂O in Acidic and Alkaline Solution and Its Catalytic Activity for Ethanol Electrooxidation, *Jurnal Sains Materi Indonesia.* **24** (2023) 81–88. <https://doi.org/10.55981/jsmi.2023.760>.
- [19] E. Achilli, A. Vertova, A. Visibile, C. Locatelli, A. Minguzzi, S. Rondinini, P. Ghigna, Structure and Stability of a Copper(II) Lactate Complex in Alkaline Solution: A Case Study by Energy-Dispersive X-ray Absorption Spectroscopy, *Inorg Chem.* **56** (2017) 6982–6989. <https://doi.org/10.1021/acs.inorgchem.7b00553>.
- [20] E. Arulkumar, S. Thanikaikarasan, N. Tesfie, Influence of Deposition Parameters for Cu₂O and CuO Thin Films by Electrodeposition Technique: A Short Review, *J Nanomater.* **2023** (2023). <https://doi.org/10.1155/2023/8987633>.
- [21] P. Poizot, C.J. Hung, M.P. Nikiforov, E.W. Bohannan, J.A. Switzer, An electrochemical method for CuO thin film deposition from aqueous solution, *Electrochemical and Solid-State Letters.* **6** (2003). <https://doi.org/10.1149/1.1535753>.
- [22] M.R. Pinto, G.B. Pereira, A.C. Queiroz, R. Nagao, Influence of the Ligands in Cu(II) Complexes on the Oscillatory Electrodeposition of Cu/Cu₂O, *Journal of Physical Chemistry C.* **124** (2020) 12559–12568. <https://doi.org/10.1021/acs.jpcc.0c02959>.
- [23] Y. Yang, M. Pritzker, Y. Li, Electrodeposited p-type Cu₂O thin films at high pH for all-oxide solar cells

- with improved performance, *Thin Solid Films*. **676** (2019) 42–53. <https://doi.org/10.1016/j.tsf.2019.02.014>.
- [24] R. Miura, R. Yuasa, T. Shinagawa, K. Fukami, K. Murase, Relationship between Copper(II)-Lactate Complexes and Cu₂O Electrodeposited Using Highly Concentrated Alkaline Solutions, *J Electrochem Soc*. **170** (2023) 092508. <https://doi.org/10.1149/1945-7111/acf792>.
- [25] K. Chen, D. Xue, pH-assisted crystallization of Cu₂O: chemical reactions control the evolution from nanowires to polyhedra, *CrystEngComm*. **14** (2012) 8068. <https://doi.org/10.1039/c2ce26084k>.
- [26] Y. Ren, J. Chen, Y. Chen, J. Chen, W. Qiu, Effects of Substrate Temperature on the Corrosion Behaviour of Nanochromium Coatings Deposited by Direct Current Magnetron Sputtering, *J Nanomater*. **2016** (2016). <https://doi.org/10.1155/2016/4894062>.
- [27] H.S. Magar, R.Y.A. Hassan, A. Mulchandani, Electrochemical Impedance Spectroscopy (EIS): Principles, Construction, and Biosensing Applications, *Sensors*. **21** (2021) 6578. <https://doi.org/10.3390/s21196578>.
- [28] T. Baran, A. Visibile, M. Busch, X. He, S. Wojtyla, S. Rondinini, A. Minguzzi, A. Vertova, Copper oxide-based photocatalysts and photocathodes: Fundamentals and recent advances, *Molecules*. **26** (2021). <https://doi.org/10.3390/molecules26237271>.
- [29] M.K. Son, Key Strategies on Cu₂O Photocathodes toward Practical Photoelectrochemical Water Splitting, *Nanomaterials*. **13** (2023). <https://doi.org/10.3390/nano13243142>.
- [30] S. Budi, D. Indrawati, M. Arum, Yusmaniar, Electrodeposition and photoelectrochemical response of Zn-doped Cu₂O, in: AIP Conf Proc, American Institute of Physics Inc., 2021. <https://doi.org/10.1063/5.0045470>.
- [31] F. Bayat, S. Sheibani, Enhancement of photocatalytic activity of CuO-Cu₂O heterostructures through the controlled content of Cu₂O, *Mater Res Bull*. **145** (2022) 111561. <https://doi.org/10.1016/j.materresbull.2021.111561>
- [32] S. Budi, D.I. Syafei, Yusmaniar, Q.F. Khasanah, D. Laxmianti, Electrodeposition of Cu₂O Films at Room Temperature for Methylene Blue Photodegradation, in: J Phys Conf Ser, Institute of Physics, 2022. <https://doi.org/10.1088/1742-6596/2377/1/012004>.